

Inorganic-organic hybrids constructed of bis(undecatungstogerma-nate)lanthanates polyoxoanions and oxalate-bridged dinuclear copper complexes and their magnetic properties

SUN Ping, MA FengJi & LIU ShuXia*

Key Laboratory of Polyoxometalates Science of Ministry of Education, College of Chemistry, Northeast Normal University, Changchun 130024, China

Received October 28, 2010; accepted November 23, 2010

A series of inorganic-organic hybrids $K_2Na_mH_{9-m}[\{Ln(GeW_{11}O_{39})_2\}\{Cu_2(bpy)_2(\mu\text{-ox})\}] \cdot nH_2O$ (bpy = 2,2-bipyridine and ox = oxalate; Ln = La, Nd, Sm, Eu, Gd; $n = 19, 17, 22, 20, 19$; $m = 4, 4, 4, 9, 2$) were isolated after reacting in a potassium acetate buffer. X-ray structural analyses show that compounds **1–5** are isomorphic and consist of $[Ln(GeW_{11}O_{39})_2]^{13-}$ polyoxoanion building blocks and oxalate-bridged dinuclear copper metalorganic complex with a 1D chain structure. The 1D chain further connects into the 3D framework by $\pi-\pi$ interactions with neighboring bpy groups. The magnetic susceptibility data indicate that anti-ferromagnetic coupling between the neighboring Cu^{2+} ions in the structure and the rare earth ions affects magnetic property of the structure.

polyoxometalates, inorganic-organic hybrid, dinuclear copper, rare earth, magnetic property

Citation: Sun P, Ma F J, Liu S X. Inorganic-organic hybrids constructed of bis(undecatungstogermanate)lanthanates polyoxoanions and oxalate-bridged dinuclear copper complexes and their magnetic properties. Chinese Sci Bull, 2011, 56: 2331–2336, doi: 10.1007/s11434-011-4488-x

Recently, the successful design and synthesis of polyoxometalates(POMs)-based hybrids has attracted considerable interest because of their diverse structures and topological properties, as well as their potential applications in catalysis [1–4]. Polyoxometalates with a strong ability to accept electrons, have been extensively used as inorganic building blocks for the construction of these materials containing organic complexes. An effective approach is to covalently link transition metal-organic ligands with POMs [5–7]. The transition-metal (TM) copper centers can have various coordination numbers and elements as well as coordination modes. They can form expansive structures by a combination of donors containing N or carboxyl groups (such as acetates and oxalates) [8,9] or by bridging Cl atoms to obtain highly nuclear magnetic clusters [10,11]. More attention has recently been given to the POM-based hybrids that have been modified by dinuclear copper com-

plexes containing carboxyl ligands. The carboxylate bridging ligand can mediate magnetic exchange interactions between metal ions [12–16]. Many oxalate-bridged dinuclear copper hybrids have been constructed using classical polyoxoanions such as the monosubstituted Keggin type $[SiW_{11}O_{39}Cu]^{6-}$ and the Anderson type $[M(OH)_7Mo_6O_{17}]^{2-}$ ($M=Al, Cr$) by Reinoso et al. [16] and our group [17]. However, the use of bis(undecatungstogermanate)lanthanates as inorganic building blocks has not been widely explored, possibly because they are difficult to assemble because of their large size. Only our group has reported a similar building block based on bis(undecatungstophosphate) lanthanates polyoxoanion inorganic-organic hybrids $K_2Na_mH_{9-m}[\{Ln(GeW_{11}O_{39})_2\}\{Cu_2(bpy)_2(\mu\text{-ox})\}] \cdot nH_2O$ (bpy = 2,2-bipyridine and ox=oxalate; Ln=La, Nd, Sm, Eu, Gd; $n = 19, 17, 22, 20, 19$; $m = 4, 4, 4, 9, 2$) by introducing dinuclear copper (II)-oxalate into the bis(undecatungstogermanate)lanthanates cluster. X-ray structural analyses show

*Corresponding author (email: liusx@nenu.edu.cn)

that compounds **1–5** are isomorphic and consist of $[\text{Ln}(\text{GeW}_{11}\text{O}_{39})_2]^{13-}$ polyoxoanion building blocks and oxalate-bridged dinuclear copper metalorganic complex with a 1D chain structure. The 1D chain further connects to the 3D framework by $\pi-\pi$ interactions of the bpy groups with neighboring chains. The magnetic susceptibility data indicate that antiferromagnetic coupling between the neighboring Cu^{2+} ions in the structure and the rare earth ions influences the magnetic property of the structure.

1 Experimental

1.1 Materials and instrumentation

The compound $\text{K}_{8-x}\text{Na}_x\text{GeW}_{11}\text{O}_{39} \cdot 9\text{H}_2\text{O}$ was prepared as previously described [19]. All the chemicals were used as purchased without further purification. Elemental analyses (C, H, and N) were performed using a Perkin-Elmer 2400 CHN elemental analyzer; Cu, W, K, Na and Ln were determined using a PLASMA-SPEC (I) ICP atomic emission spectrometer. IR spectra were recorded from 400 – 4000 cm^{-1} on an Alpha Centauri FT/IR spectrophotometer using KBr pellets. Thermal stability analyses were performed on a Perkin-Elmer TGA-7 instrument in flowing N_2 at a heating rate of 10°C/min. Magnetic susceptibility data were collected from 2–300 K under a magnetic field of 1000 Oe on a Quantum Design MPMS-5 SQUID magnetometer. Diamagnetic corrections were estimated using Pascal's constants.

1.2 Synthesis of $\text{K}_2\text{Na}_4\text{H}_5[\{\text{La}(\text{GeW}_{11}\text{O}_{39})_2\}\{\text{Cu}_2(\text{bpy})_2(\mu\text{-ox})\}] \cdot 19\text{H}_2\text{O}$ (1)

A cationic complex $[\text{Cu}_2(2,2\text{-bpy})_2(\mu\text{-ox})]^{2+}$ (**A**) and the bis(undecatungstogermanate) anion $[\text{La}(\text{GeW}_{11}\text{O}_{39})_2]^{13-}$ (**B**) were prepared. For **A**: to an aqueous solution (20 mL) of $\text{CuCl}_2 \cdot 2\text{H}_2\text{O}$ (68 mg, 0.4 mmol) were successively added a solution of 2,2-bipyridine (62 mg, 0.4 mmol) in ethanol (10 mL) and oxalic acid (25 mg, 0.2 mmol) in water (10 mL). For **B**: to an aqueous solution (20 mL) of $\text{LaCl}_3 \cdot 7\text{H}_2\text{O}$ (37 mg, 0.1 mmol) was added a solution of $\text{K}_{8-x}\text{Na}_x\text{GeW}_{11}\text{O}_{39} \cdot 9\text{H}_2\text{O}$ (610 mg, 0.2 mmol) in 1 mol/L (20 mL) potassium acetate buffer at pH 4.8. Then, solution **A** was added dropwise to solution **B** and a blue precipitate appeared. The resulting mixture was heated to 80°C for 30 min, after cooling to room temperature, and the precipitate was removed by filtration. The filtrate was allowed to stand at room temperature for crystallization. Blue block-shaped crystals of compound **1** were obtained after about a week. Yield: 60% (based on W). Elemental Anal. Calcd. for $\text{C}_{22}\text{N}_4\text{H}_{59}\text{Ge}_2\text{W}_{22}\text{LaCu}_2\text{Na}_4\text{K}_2\text{O}_{101}$ (%): C, 3.99; N, 0.85; H, 0.90; W, 61.08; La, 2.10; Cu, 1.92; K 1.18; Na 1.39. Found(%): C, 3.96; N, 0.89; H, 0.79; W, 60.05; La, 2.16; Cu, 1.88; K 1.02;

Na 1.25. IR (KBr, cm^{-1}): 3431 (br), 1641 (m), 1600 (m), 1496 (m), 1473 (m), 1446 (m), 1315 (m), 1171 (m), 1100 (m), 943 (m), 881 (s), 818 (s), 755 (s), 728 (m), 528 (m), 467 (m).

1.3 Synthesis of $\text{K}_2\text{Na}_4\text{H}_5[\{\text{Nd}(\text{GeW}_{11}\text{O}_{39})_2\}\{\text{Cu}_2(\text{bpy})_2(\mu\text{-ox})\}] \cdot 17\text{H}_2\text{O}$ (2)

The synthesis of compound **2** followed the procedure described above except that $\text{LaCl}_3 \cdot 7\text{H}_2\text{O}$ was replaced by NdCl_3 (25 mg, 0.1 mmol). Yield: 61% (based on W). Elemental Anal. Calcd. for $\text{C}_{22}\text{N}_4\text{H}_{55}\text{Ge}_2\text{W}_{22}\text{NdCu}_2\text{Na}_4\text{K}_2\text{O}_{99}$ (%): C, 4.01; N, 0.85; H, 0.84; W, 61.36; Nd, 2.19; Cu, 1.93; K 1.19; Na 1.40. Found (%): C, 4.23; N, 0.79; H, 0.95; W, 59.51; Nd, 2.35; Cu, 1.76; K 1.22; Na 1.15. IR (KBr, cm^{-1}): 3423 (br), 1642 (m), 1600 (m), 1496 (m), 1472 (m), 1445 (m), 1314 (m), 1169 (m), 1100 (m), 946 (m), 872 (s), 816 (s), 755(s), 719 (m), 526 (m), 466 (m).

1.4 Synthesis of $\text{K}_2\text{Na}_4\text{H}_5[\{\text{Sm}(\text{GeW}_{11}\text{O}_{39})_2\}\{\text{Cu}_2(\text{bpy})_2(\mu\text{-ox})\}] \cdot 22\text{H}_2\text{O}$ (3)

The synthesis of **3** followed the procedure described above except that $\text{LaCl}_3 \cdot 7\text{H}_2\text{O}$ was replaced by SmCl_3 (26 mg, 0.1 mmol). Yield: 55% (based on W). Elemental Anal. Calcd. for $\text{C}_{22}\text{N}_4\text{H}_{65}\text{Ge}_2\text{W}_{22}\text{SmCu}_2\text{Na}_4\text{K}_2\text{O}_{104}$ (%): C, 3.95; N, 0.84; H, 0.98; W, 60.48; Sm, 2.25; Cu, 1.90; K 1.17; Na 1.38. Found (%): C, 3.97; N, 0.91; H, 0.92; W, 58.48; Sm, 2.03; Cu, 2.12; K 1.29; Na 1.22. IR (KBr, cm^{-1}): 3423 (br), 1640 (m), 1600 (m), 1496 (m), 1471 (m), 1445 (m), 1312 (m), 1170 (m), 1100 (m), 944 (m), 872 (s), 818 (s), 756 (s), 728 (m), 523 (m), 467 (m).

1.5 Synthesis of $\text{K}_2\text{Na}_9[\{\text{Eu}(\text{GeW}_{11}\text{O}_{39})_2\}\{\text{Cu}_2(\text{bpy})_2(\mu\text{-ox})\}] \cdot 20\text{H}_2\text{O}$ (4)

The synthesis of **4** followed the procedure described above except that $\text{LaCl}_3 \cdot 7\text{H}_2\text{O}$ was replaced by EuCl_3 (26 mg, 0.1 mmol). Yield: 57% (based on W). Elemental Anal. Calcd. for $\text{C}_{22}\text{N}_4\text{H}_{56}\text{Ge}_2\text{W}_{22}\text{EuCu}_2\text{Na}_9\text{K}_2\text{O}_{102}$ (%): C, 3.91; N, 0.83; H, 0.83; W, 59.81; Eu, 2.25; Cu, 1.88; K 1.16; Na 3.06. Found(%): C, 3.86; N, 0.96; H, 0.95; W, 62.23; Eu, 2.01; Cu, 1.79; K 1.03; Na 2.85. IR (KBr, cm^{-1}): 3422 (br), 1638 (m), 1600 (m), 1496 (m), 1472 (m), 1446 (m), 1313 (m), 1170 (m), 1100 (m), 944 (m), 871 (s), 818 (s), 755 (s), 728 (m), 520 (m), 467 (m).

1.6 Synthesis of $\text{K}_2\text{Na}_2\text{H}_7[\{\text{Gd}(\text{GeW}_{11}\text{O}_{39})_2\}\{\text{Cu}_2(\text{bpy})_2(\mu\text{-ox})\}] \cdot 19\text{H}_2\text{O}$ (5)

The synthesis of **5** followed the procedure described above except that $\text{LaCl}_3 \cdot 7\text{H}_2\text{O}$ was replaced by GdCl_3 (26 mg, 0.1 mmol). Yield: 52% (based on W). Elemental Anal. Calcd. for $\text{C}_{22}\text{N}_4\text{H}_{61}\text{Ge}_2\text{W}_{22}\text{GdCu}_2\text{Na}_2\text{K}_2\text{O}_{101}$ (%): C, 4.01; N, 0.85; H, 0.93; W, 61.32; Gd, 2.38; Cu, 1.93; K 1.19; Na 0.70.

Found (%): C, 3.94; N, 0.81; H, 0.97; W, 63.82; Gd, 2.40; Cu, 1.90; K 1.29; Na 0.53. IR (KBr, cm^{-1}): 3431 (br), 1637 (m), 1600 (m), 1496 (m), 1473 (m), 1439 (m), 1314 (m), 1113 (m), 1100 (m), 943 (m), 869 (s), 819 (s), 755 (s), 711 (m), 528 (m), 465 (m).

1.7 X-ray single crystal diffraction analysis

The diffraction intensities for compounds **2**, **3** and **5** were collected on a SMART CCD diffractometer (Rigaku R-AXISRAPID IP diffractometer for **1** and **4**) equipped with a graphite monochromatic Mo-K α radiation source ($\lambda = 0.71073 \text{ \AA}$) at 293 K. The structures were solved by the direct method and refined by the full-matrix least-squares method on F^2 using the SHELXTL crystallographic software package [20]. The hydrogen atoms were placed geometrically on the 2,2'-bipyridine ligands.

2 Results and discussion

2.1 Synthesis and structure

Compounds **1–5** were successfully isolated after the solution reaction of $[\text{Cu}_2(\text{bpy})_2(\mu\text{-ox})]^{2+}$ and bis(undecatungstogermanate) $[\text{Ln}(\text{GeW}_{11}\text{O}_{39})_2]^{13-}$. It is worth noting that the role

of the potassium acetate buffer as an agent can be confirmed by the formation of bis(undecatungstogermanate) $[\text{Ln}(\text{GeW}_{11}\text{O}_{39})_2]^{13-}$ polyoxoanions. When the reaction was carried out without a potassium acetate buffer, the M/ $[\alpha\text{-GeW}_{11}\text{O}_{39}]$ (M = Nd, Sm, Y, Yb) series of compounds formed [21]. It is obvious that the steady pH provided by the buffer solution is significant.

Single-crystal X-ray diffraction analysis revealed that compounds **1–5** are isomorphic only with slight differences in bond length, bond angle and the amount of lattice water (Table 1). Compound **1** is described as an example below. Compound **1** consists of $[\text{Cu}_2(\text{bpy})_2(\mu\text{-ox})]^{2+}$, $[\text{La}(\text{GeW}_{11}\text{O}_{39})_2]^{13-}$ and water molecules that are located inside the framework between the adjacent chains. The central Ln (III) ions are coordinated to eight unsaturated O atoms from the asymmetry of two $[\alpha\text{-GeW}_{11}\text{O}_{39}]^{8-}$ ions and they exhibit a twisted square antiprismatic coordination geometry in the $[\text{La}(\text{GeW}_{11}\text{O}_{39})_2]^{13-}$ unit. In compounds **1–5**, the bond lengths of Ln-O_{POM} (La-Gd) vary from 2.552 to 2.394 \AA (Table 2) along with a decrease in lanthanide ion size, which corresponds to the lanthanide contraction effect [22]. The centrosymmetric $[\text{Cu}_2(\text{bpy})_2(\mu\text{-ox})]^{2+}$ consists of two copper atoms bridged by an oxalate in a bis-bidentate fashion. Each of the copper atoms is six-coordinated in a contorted octahedral coordination geometry, and they are

Table 1 Crystal data and structure refinement parameters for compounds **1–5**

| | 1 | 2 | 3 | 4 | 5 |
|---------------------------------------------------------------------------|------------------------------------------------------------------------------------------------------------------|-------------------------------------------------------------------------------------------------------------------|-------------------------------------------------------------------------------------------------------------------|-------------------------------------------------------------------------------------------------------------------|-------------------------------------------------------------------------------------------------------------------|
| Empirical formula | $\text{C}_{22}\text{N}_4\text{H}_{55}\text{Ge}_2\text{W}_{22}\text{LaCu}_{2-}\text{Na}_4\text{K}_2\text{O}_{99}$ | $\text{C}_{22}\text{N}_4\text{H}_{59}\text{Ge}_2\text{W}_{22}\text{NdCu}_{2-}\text{Na}_4\text{K}_2\text{O}_{101}$ | $\text{C}_{22}\text{N}_4\text{H}_{65}\text{Ge}_2\text{W}_{22}\text{SmCu}_{2-}\text{Na}_4\text{K}_2\text{O}_{104}$ | $\text{C}_{22}\text{N}_4\text{H}_{56}\text{Ge}_2\text{W}_{22}\text{EuCu}_{2-}\text{Na}_9\text{K}_2\text{O}_{102}$ | $\text{C}_{22}\text{N}_4\text{H}_{61}\text{Ge}_2\text{W}_{22}\text{GdCu}_{2-}\text{Na}_2\text{K}_2\text{O}_{101}$ |
| <i>M</i> | 6585.55 | 6626.92 | 6687.08 | 6762.57 | 6595.96 |
| Crystal system | Monoclinic | Monoclinic | Monoclinic | Monoclinic | Monoclinic |
| Space group | <i>C</i> 2/c | <i>C</i> 2/c | <i>C</i> 2/c | <i>C</i> 2/c | <i>C</i> 2/c |
| θ range($^\circ$) | 3.00–25.00 | 1.09–25.00 | 1.09–25.00 | 3.01–25.01 | 1.09–25.00 |
| <i>a</i> (\AA) | 15.737(3) | 15.920(2) | 15.8644(13) | 15.963(3) | 15.6336(13) |
| <i>b</i> (\AA) | 19.923(4) | 20.038(2) | 20.0581(13) | 19.965(4) | 20.0523(13) |
| <i>c</i> (\AA) | 37.805(8) | 38.106(5) | 38.060(3) | 37.694(8) | 38.027(3) |
| α ($^\circ$) | 90.00(0) | 90.00(0) | 90.00(0) | 90.00(0) | 90.00(0) |
| β ($^\circ$) | 101.69(3) | 101.981(2) | 101.8660(10) | 101.74(3) | 101.5860(10) |
| γ ($^\circ$) | 90.00(0) | 90.00(0) | 90.00(0) | 90.00(0) | 90.00(0) |
| <i>V</i> (\AA^3) | 11607(4) | 11891(2) | 11852.3(16) | 11762(4) | 11678.2(15) |
| <i>Z</i> | 4 | 4 | 4 | 4 | 4 |
| <i>F</i> (000) | 11748.0 | 11440.0 | 11424.0 | 11864.0 | 11336.0 |
| <i>D</i> _c (g cm^{-3}) | 3.838 | 3.660 | 3.667 | 3.823 | 3.698 |
| Abs coeff (mm^{-1}) | 23.130 | 22.644 | 22.769 | 23.010 | 23.171 |
| Total data collected | 44497 | 29976 | 29939 | 44165 | 29419 |
| Unique data | 10227 | 10463 | 10435 | 10364 | 10283 |
| <i>R</i> _{int} | 0.1191 | 0.076 | 0.0682 | 0.1226 | 0.0703 |
| GOF | 1.027 | 1.043 | 1.052 | 1.063 | 1.057 |
| <i>R</i> ₁ [<i>I</i> > 2 <i>σ</i> (<i>I</i>)] ^{a)} | 0.0574 | 0.0537 | 0.0518 | 0.0562 | 0.0543 |
| w <i>R</i> ₂ (all data) ^{b)} | 0.1253 | 0.1434 | 0.1384 | 0.0922 | 0.1444 |

a) $R_1 = \sum |F_o| - |F_c| / \sum |F_o|$; b) $wR_2 = [\sum w(F_o^2 - F_c^2)^2 / \sum w(F_o^2)]^{1/2}$.

Table 2 Ln–O bond lengths in compounds **1–5**

| Compound | Ln–O bond length |
|-------------------------------|------------------|
| 1 (La^{3+}) | 2.526–2.552 |
| 2 (Nd^{3+}) | 2.440–2.507 |
| 3 (Sm^{3+}) | 2.403–2.479 |
| 4 (Eu^{3+}) | 2.398–2.467 |
| 5 (Gd^{3+}) | 2.394–2.464 |

connected by two oxalate oxygen atoms and two bipyridine nitrogen atoms at the equatorial positions and two terminal oxygen atoms from the $[\text{Ln}(\text{GeW}_{11}\text{O}_{39})_2]^{13-}$ polyoxoanions at the axial positions with a Cu–Cu distance close to the average of 5.2 Å. The connection between $[\text{Cu}_2(\text{bpy})_2(\mu\text{-ox})]^{2+}$ and $[\text{La}(\text{GeW}_{11}\text{O}_{39})_2]^{13-}$ gives a 1D chain (Figure 1). Adjacent bipyridine layers further result in a 3D structure by π – π stacking interactions (distance between the bpy layers are approximately 3.7 Å) (Figure 2).

2.2 IR spectroscopy

The IR spectra of compounds **1–5** are similar, as shown in Figure 3, there are 4 characteristic asymmetric vibrations that result from the $[\text{Ln}(\text{GeW}_{11}\text{O}_{39})_2]^{13-}$ polyoxoanions, namely, mas(W–O_a), mas(W–O_b), mas(W–O_c) and mas(Ge–O_a) that appear at 943, 872, 755 and 816 cm⁻¹, respectively. By comparing the IR spectra of the polyoxoanions with those of $\alpha\text{-H}_4\text{GeW}_{12}\text{O}_{40}$ [23], shifts and splits are present

because of the lower symmetry. The characteristic peaks that are present between 1100 and 1600 cm⁻¹ are attributed to the 2,2'-bipyridine ligand, and these are of low intensity with respect to those of the polyoxoanions. The features at about 755 cm⁻¹ are assigned to ν_{as} (CO) and those at 1315 and 1360 cm⁻¹ are assigned to ν_s (CO) while the broad absorption at 1642 cm⁻¹ corresponds to $\nu(\text{OCO})$ of the oxalate ligand in bisbidentate bridging mode [24].

2.3 Thermogravimetric analyses

For compounds **1–5**, the amount of lattice water was determined by thermal gravimetric analysis. The curve of compound **1** gives a total weight loss of 11.69% between 25–750°C, which agrees with the calculated value of 11.85%. The weight loss of 5.17% at 25–260°C corresponds to the loss of all non-coordinated and coordinated water molecules (calcd. 5.19%). The weight loss of 6.52% at 260–750°C arises from the decomposition of organic molecules (calcd. 6.66%). Compounds **2–5** also undergo a two-step weight loss.

2.4 Magnetic properties

Oxalate dinuclear copper compounds are known to exhibit strong antiferromagnetic interactions [25]. When rare earth ions are added to the dinuclear compounds, the crystal

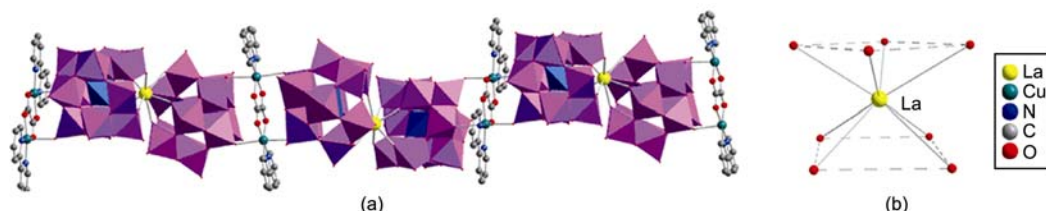


Figure 1 1D structure of compound **1** and the coordination mode of La ion.

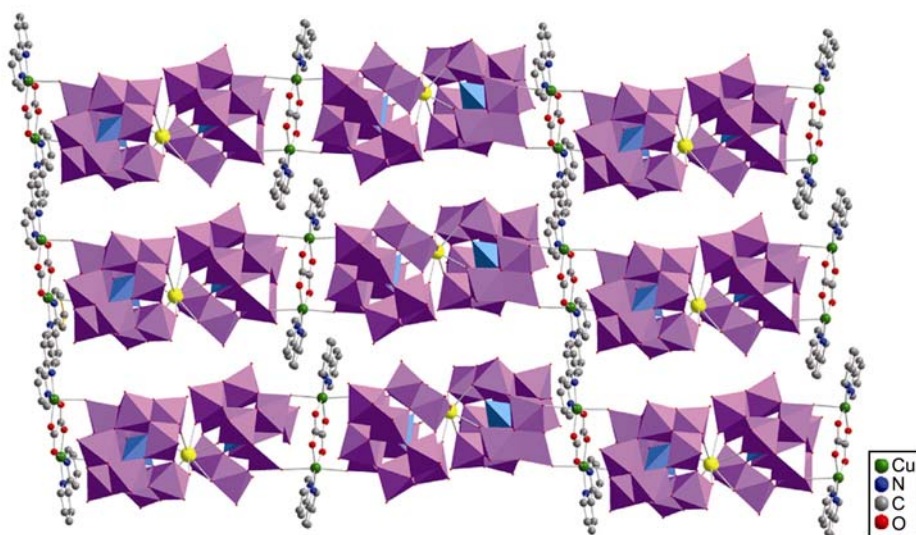


Figure 2 3D structure of compound **1**.

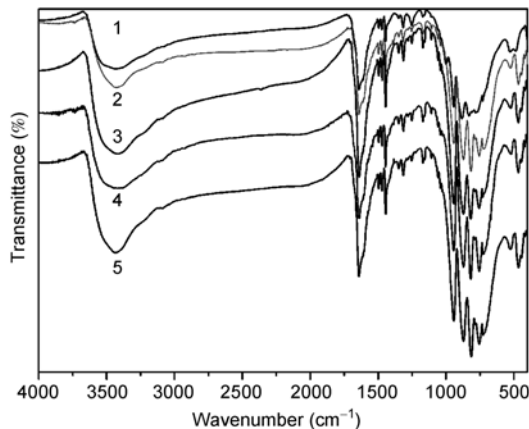


Figure 3 IR spectrum of compounds **1–5**.

structure becomes complex as the two copper (II) ions and the free Ln^{3+} make the analysis of the observed magnetic behavior difficult. For example, despite the presence of strong antiferromagnetic interactions, no relative maximum is observed on the susceptibility versus temperature curve. It is possible that the expected maximum is outside the measured temperature range but it is also possible that the maximum is enveloped by the contributions of the $\text{Ln}(\text{III})$ ions. According to the change in the rare earth ion f-orbital electronic number from zero to partially full to half full, the thermal evolution of the magnetic molar susceptibility and the $\chi_m T$ product of **1**, **2** and **5** in the temperature range 2–300 K are shown selectively in Figure 4. For compound **1**, from 300 to 2 K, the χ_m value increases gradually with a decrease in temperature and no maximum is observed. The $\chi_m T$ value is equal to $0.609 \text{ cm}^3 \text{ K mol}^{-1}$ at 300 K, which is lower than the expected value of $0.750 \text{ cm}^3 \text{ K mol}^{-1}$ for the two $S = 1/2 \text{ Cu}^{2+}$ centers with $\chi_m T = \mu_{\text{eff}}^2 / 8$ (considering $g = 2$). Upon cooling the samples, the product $\chi_m T$ decreases from 300 to 50 K, and $\chi_m T$ remains constant around 0.0869 $\text{cm}^3 \text{ K mol}^{-1}$ when the temperature is lower than 50 K and this may be attributed to a paramagnetic impurity. The decrease in $\chi_m T$ indicates the antiferromagnetic coupling of the bridged-oxalate dinuclear copper; and the rare earth ion (La^{3+} , $4f^0$) does not contribute to the magnetic property of the whole structure. Thus the oxalate-bridged dinuclear copper complex has intrinsic magnetism in the inorganic-organic hybrids. For compound **2**, the $\chi_m T$ curve is different to that of the former because of the existence of paramagnetic Nd^{3+} ions. This fact indicates the predominance of antiferromagnetic interactions in compound **2**, as confirmed by the rapid decrease in the effective magnetic moment with a decrease in temperature from 300 to 2 K. Moreover, the exchange coupling must certainly be strong considering that Curie-Weiss behavior is not observed even at a high temperature on the reciprocal susceptibility curve. The $\chi_m T$ value at room temperature is equal to $1.789 \text{ cm}^3 \text{ K mol}^{-1}$, which is lower than the expected value of 2.386

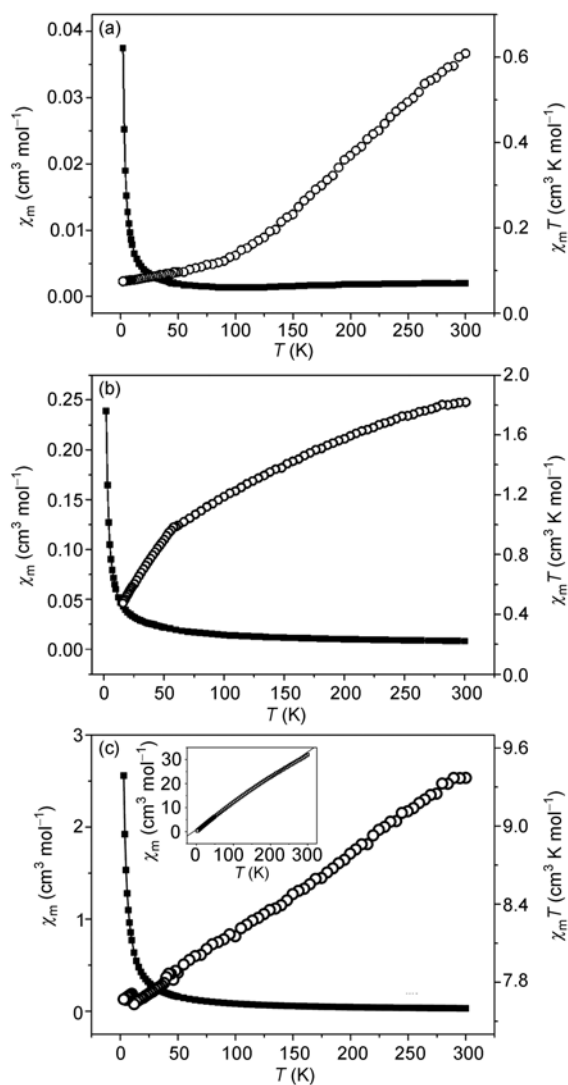


Figure 4 Temperature dependence of magnetic susceptibility of compounds **1**, **2** and **5** are (a), (b), (c), respectively.

$\text{cm}^3 \text{ K mol}^{-1}$ for two $S = 1/2 \text{ Cu}^{2+}$ centers with $\chi_m T = \mu_{\text{eff}}^2 / 8$ (considering $g = 2$) and one free Nd^{3+} ion in the ${}^4\text{I}_{9/2}$ ground state ($g' = 8/11$). Upon cooling the samples, the product $\chi_m T$ decreases very sharply and reaches a minimum ($0.475 \text{ cm}^3 \text{ K mol}^{-1}$) at 2 K, and this may be attributed to crystal field effects because of the intrinsic nature of the lanthanide series [26]. For compound **5**, the magnetic coupling is dependent on the exchange transfer integral between the 3d orbital of Cu (II) and the 4f orbital of Gd (III); however, the long Cu–Gd distance (10.527 \AA) may affect the magnetic interactions in the whole structure. According to the Curie-Weiss law, there is a dominant antiferromagnetic coupling in oxalate-bridging Cu(II) dimers. Similar magnetic curves were found for compounds **2** and **5**. For compound **5**, the $\chi_m T$ curve is different to that of the former because of the existence of half-full Gd^{3+} ($4f^7$) ions. The relationship between $1/\chi_m$ and T from 2–300 K fits the Curie-Weiss law

($\chi_m = C/(T-\theta)$), giving $C = 9.2989 \text{ cm}^3 \text{ K mol}^{-1}$ and $\theta = -7.9092 \text{ K}$. The negative Weiss constant indicates that a dominant antiferromagnetic coupling exists in the structure. The $\chi_m T$ value at room temperature is $9.140 \text{ cm}^3 \text{ K mol}^{-1}$, which is higher than the expected value of $8.625 \text{ cm}^3 \text{ K mol}^{-1}$ for the two $S = 1/2$ ($\chi_m T = 0.750$) Cu^{2+} centers with $\chi_m T = \mu_{\text{eff}}^2/8$ (considering $g = 2$) and one $S = 7/2$ ($\chi_m T = 7.875$) free Gd^{3+} ion in the ${}^8S_{7/2}$ ground state ($g' = 2$). Upon cooling the samples, the product $\chi_m T$ decreases continually from 300 K to 2 K in a near straight line because the rare earth ions play a role in the magnetic character of this structure.

3 Conclusions

In this paper, we synthesized five novel inorganic-organic hybrid compounds using bis(undecatungstogermanate) and oxalate-bridged dinuclear copper complexes by conventional methods. Magnetic susceptibility studies reveal a strong antiferromagnetic coupling in the dinuclear copper complexes and the choice of different rare earth ions affects the magnetic property of the structure.

- 1 Gouzerh P, Proust A. Main-Group element, organic, and organometallic derivatives of polyoxometalates. *Chem Rev*, 1998, 98: 77–111
- 2 Kitaura R, Kitagawa S, Kubota Y, et al. Formation of a one-dimensional array of oxygen in a microporous metal-organic solid. *Science*, 2002, 298: 2358–2361
- 3 Sun C Y, Liu S X, Liang D D, et al. Highly stable crystalline catalysts based on a microporous metal-organic framework and polyoxometalates. *J Am Chem Soc*, 2009, 131: 1883–1888
- 4 Hagman P J, Hagman D, Zubietta J. Organic-inorganic hybrid materials: From simple coordination polymers to organodiamine-templated molybdenum oxides. *Angew Chem Int Ed*, 1999, 38: 2638–2684
- 5 Liu S X, Xie L H, Gao B, et al. An organic-inorganic hybrid material constructed from a three-dimensional coordination complex cationic framework and entrapped hexadecavanadate clusters. *Chem Commun*, 2005, 5023–5025
- 6 Zhao X, Liang D, Liu S, et al. Two Dawson-templated three-dimensional metal-organic frameworks based on oxalate-bridged binuclear cobalt(II)/nickel(II) SBUs and bpy linkers. *Inorg Chem*, 2008, 10: 7133–7138
- 7 Reinoso S, Vitoria P, Felices L S, et al. Tetrahydroxy-p-benzoquinone as a source of polydentate O-donor ligands: Synthesis, crystal structure, and magnetic properties of the $[\text{Cu}(\text{bpy})(\text{dhmal})_2]$ dimer and the two-dimensional $[\{\text{SiW}_{12}\text{O}_{40}\}\{\text{Cu}_2(\text{bpy})_2(\text{H}_2\text{O})(\text{ox})\}_2] \cdot 16\text{H}_2\text{O}$ inorganic-metalorganic hybrid. *Inorg Chem*, 2007, 46: 1237–1249
- 8 Pichon C, Mialane P, Dolbecq A, et al. Characterization and electrochemical properties of molecular icosanuclear and bidimensional hexanuclear Cu(II) azido Polyoxometalates. *Inorg Chem*, 2007, 46: 5292–5301
- 9 Felices L S, Vitoria P, Gutiérrez-Zorrilla J M, et al. A novel hybrid inorganic-metalorganic compound based on a polymeric polyoxometalate and a copper complex: Synthesis, crystal structure and topological studies. *Chem Eur J*, 2004, 10: 5138–5146
- 10 Zhang C D, Liu S X, Sun C Y, et al. Assembly of organic-inorganic hybrid materials based on Dawson-type polyoxometalate and multi-nuclear copper-phen complexes with unique magnetic properties. *Cryst Growth Des*, 2009, 9: 3655–3660
- 11 Yang H X, Guo S P, Tao J, et al. Hydrothermal syntheses, crystal structures, and magnetic properties of a series of complexes constructed from multinuclear copper clusters and polyoxometalates. *Cryst Growth Des*, 2009, 9: 4735–4744
- 12 Ushak S, Spodine E, Fur E, et al. Two new hybrid organic/inorganic copper(II)-oxovanadate(V)diphosphonates $[\text{Cu}_2(\text{phen})_2(\text{O}_3\text{PCH}_2\text{PO}_3)(\text{V}_2\text{O}_5)(\text{H}_2\text{O})] \cdot \text{H}_2\text{O}$ and $[\text{Cu}_2(\text{phen})_2(\text{O}_3\text{P}(\text{CH}_2)\text{PO}_3)(\text{V}_2\text{O}_5)] \cdot \text{C}_3\text{H}_8$: Synthesis, structure, and magnetic properties. *Inorg Chem*, 2006, 45: 5393–5398
- 13 Reinoso S, Vitoria P, Gutiérrez-Zorrilla J M, et al. Inorganic-metalorganic hybrids based on copper(II)-monosubstituted Keggin polyanions and dinuclear copper(II)-oxalate complexes: Synthesis, X-ray structural characterization, and magnetic properties. *Inorg Chem*, 2005, 44: 9731–9742
- 14 Reinoso S, Vitoria P, Lezama L, et al. A novel organic-inorganic hybrid based on a dinuclear copper complex supported on a Keggin polyoxometalate. *Inorg Chem*, 2003, 42: 3709–3711
- 15 Reinoso S, Vitoria P, Gutiérrez-Zorrilla J M, et al. Coexistence of five different copper(II)-phenanthroline species in the crystal packing of inorganic-metalorganic hybrids based on Keggin polyoxometalates and copper(II)-phenanthroline-oxalate complexes. *Inorg Chem*, 2007, 46: 4010–4021
- 16 Reinoso S, Vitoria P, Felices L S, et al. Analysis of weak interactions in the crystal packing of inorganic metalorganic hybrids based on Keggin polyoxometalates and dinuclear copper(II)-acetate complexes. *Inorg Chem*, 2006, 45: 108–118
- 17 Cao R G, Liu S X, Xie L H, et al. Organic-inorganic hybrids constructed of Anderson-type polyoxoanions and oxalato-bridged dinuclear copper complexes. *Inorg Chem*, 2007, 46: 3541–3547
- 18 Cao J F, Liu S X, Cao R G, et al. Organic-inorganic hybrids assembled by bis(undecatungstophosphate) lanthanates and dinuclear copper(II)-oxalate complexes. *Dalton Trans*, 2008, 115–120
- 19 Haraguchi N, Okabe Y, Isobe T, et al. Stabilization of tetravalent cerium upon coordination of unsaturated heteropolytungstate anions. *Inorg Chem*, 1994, 33: 1015–1020
- 20 Sheldrick G M. SHELXS-97. Program for Crystal Structure Solution. Göttingen, Germany: University of Göttingen, 1997
- 21 Wang J P, Duan X Y, Du X D, et al. Novel rare earth germanotungstates and organic hybrid derivatives: Synthesis and structures of $M/[\alpha\text{-GeW}_{11}\text{O}_{39}]$ ($M = \text{Nd}, \text{Sm}, \text{Y}, \text{Yb}$) and $\text{Sm}/[\alpha\text{-GeW}_{11}\text{O}_{39}](\text{DMSO})$. *Cryst Growth Des*, 2006, 6: 2266–2270
- 22 Gaunt A J, May I, Sarsfield M J, et al. A rare structural characterisation of the phosphomolybdate lacunary anion, $[\text{PMo}_{11}\text{O}_{39}]^{7-}$ crystal structures of the $\text{Ln}(\text{III})$ complexes, $(\text{NH}_4)_{11}[\text{Ln}(\text{PMo}_{11}\text{O}_{39})_2] \cdot 16\text{H}_2\text{O}$ ($\text{Ln} = \text{Ce}^{\text{III}}, \text{Sm}^{\text{III}}, \text{Dy}^{\text{III}}$ or Lu^{III}). *Dalton Trans*, 2003, 2767–2771
- 23 Rocchiccioli-Deltcheff C, Fournier M, Franck R, et al. Vibrational investigations of polyoxometalates. 2. evidence for anion-anion interactions in molybdenum(VI) and tungsten(VI) compounds related to the Keggin structure. *Inorg Chem*, 1983, 22: 207–216
- 24 Thomas A M, Mandal G C, Tiwary S K, et al. Ascorbate oxidation leading to the formation of a catalytically active oxalato bridged di-copper(II) complex as a model for dopamine β -hydroxylase. *J Chem Soc Dalton Trans*, 2000, 1395–1396
- 25 Alvarez S, Julve M, Verdaguera M. Oxalato-bridged and related dinuclear copper(III) complexes: Theoretical analysis of their structures and magnetic coupling. *Inorg Chem*, 1990, 29: 4500
- 26 Wu A Q, Zheng F K, Chen W T, et al. Two series of novel rare earth complexes with dicyanamide $[\text{Ln}(\text{dca})_2(\text{phen})_2(\text{H}_2\text{O})_3][\text{dca}] \cdot (\text{phen})$, ($\text{Ln} = \text{Pr}, \text{Gd}$, and Sm) and $[\text{Ln}(\text{dca})_3(2,2\text{-bipy})_2(\text{H}_2\text{O})]_n$, ($\text{Ln} = \text{Gd}, \text{Sm}$, and La): Syntheses, crystal structures, and magnetic properties. *Inorg Chem*, 2004, 43: 4839–4845